SSRG International Journal of Electrical and Electronics Engineering
ISSN: 2348-8379/ https://doi.org/10.14445/23488379/IJEEE-V11I12P127

Volume 11 Issue 12, 295-301, December 2024

Original Article

An Adaptive Active Disturbance Rejection Controller (ADRC) for Induction Motor Drives

Vo Quang Vinh[1*], Trịnh Cao Phat[2], Nguyễn Hữu Giang[3]

[1]*Electric Power University, Hanoi 100000, Vietnam*
[2]*Le Hong Phong High School for the Gifted, Vietnam*
[3]*Hanoi University of Industry, Vietnam*

[*]*Corresponding Author : vinhvq@epu.edu.vn*

Received: 15 October 2024 Revised: 16 November 2024 Accepted: 14 December 2024 Published: 31 December 2024

Abstract - *The paper explores enhancing the torque response of the Induction Motor (IM) drive systems using Adaptive Active Disturbance Rejection Control (ADRC). The ADRC structure comprises three key components: the Tracking Differentiator (TD) for generating a smooth reference signal, the Extended State Observer (ESO) for estimating system states and disturbances, and Nonlinear State Error Feedback (NLSEF) for adjusting the output based on state errors. This approach allows ADRC to effectively manage nonlinear drive systems without requiring an exact model while improving resilience to disturbances and uncertainties. Performance improvements and reductions in torque pulsation are validated through MATLAB simulations.*

Keywords - *Induction motor, IM, ADRC controller, PI controller.*

1. Introduction

Induction motor drive systems are widely used for domestic and international electric vehicles [1]. Therefore, improving the electric drive system and torque control is crucial. This improves acceleration and braking capabilities and enhances stability and handling. The system helps electric cars operate more efficiently in different situations while saving energy by adjusting the motor torque according to specific requirements [2-4].

Through the survey, the author found that more published research works on solutions to improve torque response for IM drive systems to ensure the performance and efficiency of the system. According to the document, the PID controller adjusts the torque by changing the current based on the error between the actual and desired current. This controller is characterised by being easy to design and implement. However, the performance can be affected by noise and changes in system parameters. Therefore, the LQR controller is suggested to replace the PID controller. In another research paper [7], ADRC, thanks to the ESO state estimation observer, adjusts the system output based on the state error (NLSEF). Therefore, ADRC can handle nonlinear systems well, does not require an exact system model, and can improve the system's robustness against disturbances and uncertainties. This is a powerful tool for controlling complex systems, especially in applications where the exact model of the system is difficult to determine, complex, or there are many disturbances [8].

On the other hand, nonlinear control, such as sliding, controls the system, making the system stable and robust against disturbances and parameter changes. However, sliding mode control has a sign function that causes chattering (vibration) in the system [9]. In addition, the Model Predictive Control (MPC) method, which uses a mathematical model of the system to predict future behaviour and optimise control, is also a popular suggestion. Although MPC can handle constraints and optimise performance, it requires high computation and is complex in design [10]. Based on the literature [11], the control parameters can be adjusted in real time to adapt to changes in the system. This solution allows the ability to adapt to changing operating conditions but is complex in design and requires high computation. This research finds that each method has advantages and disadvantages, and the choice of method depends on the application's specific requirements, the system's computational capacity, and the level of complexity that the designer can accept.

This paper proposes using ADRC control to enhance the torque response of a sensorless IM drive system. The system replaces the speed sensor with a slip observer integrated with a neural network to estimate speed and flux, reducing hardware costs and complexity. This approach addresses system uncertainties, external disturbances, and model inaccuracies, such as load variations, while improving electric vehicle speed control, energy efficiency, and overall motor reliability [12-114]. ADRC provides a robust alternative to

traditional PID controllers by compensating for dynamic uncertainties and disturbances, ensuring better torque stability and faster transient response. The slip observer with a neural network further enhances adaptability by learning and predicting the motor's non-linear dynamics, reducing reliance on physical sensors and improving speed and flux estimation accuracy critical for sensorless IM applications.

The paper is organised into five sections. It begins by highlighting the issue's urgency and reviewing torque control methods for Induction Motors (IMs) in electric vehicles. It then introduces the IM mathematical model, followed by the design of ADRC and PI controllers using current and speed models. MATLAB simulations demonstrate the superior performance of the ADRC controller compared to the PI controller. The paper concludes with findings and recommendations for improving IM torque control, addressing real-world challenges such as the PI controller's limitations in handling parameter variations and disturbances. ADRC is proposed as a robust alternative capable of real-time compensation for uncertainties and disturbances.

2. Mathematical Modelling of an IM Motor

Based on [14], a mathematical model of an IM motor is essential for designing control strategies and simulating motor behaviours in real-world applications. This model is typically represented in the *dq*-reference frame, also known as the rotating reference frame. This frame simplifies the analysis of three-phase AC motors by converting them into a two-axis system.

Voltage Equations in *dq*-reference frame*:* The mathematical model of an IM motor in the *dq*-reference frame is derived from the stator voltage equations. These equations describe the dynamics of the stator windings and are represented along two orthogonal axes: the direct axis (d-axis) and the quadrature axis (q-axis).

2.1. Stator Voltage Equations

$$u_d = R_s i_d + L_d \frac{di_d}{dt} - \omega_r L_q i_q \quad (1)$$

$$u_q = R_s i_q + L_q \frac{di_q}{dt} + \omega_e L_d i_d + \omega_r \varphi_f \quad (2)$$

Where**:** u_d, u_q are voltages in the d-axis, q-axis (V); i_d, i_q are currents in the d-axis, q-axis (A); L_d, L_q are inductances in the d-axis and q-axis (H); φ_f is permanent magnet flux linkage (Wb) permanent magnet flux linkage (Wb); ω_r is the electrical angular velocity of the rotor (rad/s).

2.2. Flux Linkage Equations

The stator flux linkages in the *dq*-reference frame can be described as:

$$\varphi_d = L_d i_d + \varphi_f \quad (3)$$

$$\varphi_q = L_q i_q \quad (4)$$

Where: φ_d, φ_q are flux linkages in the d-axis and q-axis (Wb)

2.3. Electromagnetic Torque Equation

The electromagnetic torque generated by the PMSM can be expressed as:

$$T_m = \frac{3}{2} p(\varphi_d i_d + \varphi_q i_q) \quad (5)$$

2.4. Mechanical Dynamics

The mechanical dynamics of the motor are governed by Newton's second law of rotation. The relationship between the torque and rotor speed can be expressed as:

$$T_m - T_L = \frac{Jd\omega_r}{dt} \quad (6)$$

Where: T_m, T_L are motor and load torques.

An IM motor state-space model is expressed as Equations (7) and (8). It provides a comprehensive and compact representation of the motor's dynamics, enabling more sophisticated control strategies.

$$\frac{d}{dt}\begin{bmatrix} i_d \\ i_q \\ \omega_r \end{bmatrix} = \begin{bmatrix} -\frac{R_s}{L_d} & \omega_r \frac{R_s}{L_d} & 0 \\ -\omega_r \frac{L_d}{L_q} & -\frac{R_s}{L_d} & -\frac{p\varphi_f}{L_q} \\ 0 & \frac{3p\varphi_f}{2J} & 0 \end{bmatrix} \begin{bmatrix} i_d \\ i_q \\ \omega_r \end{bmatrix} + \begin{bmatrix} -\frac{1}{L_d} & 0 \\ 0 & \frac{1}{L_q} \\ 0 & 0 \end{bmatrix} \begin{bmatrix} u_d \\ u_q \end{bmatrix} \quad (7)$$

$$\begin{bmatrix} \omega_r \\ T_m \end{bmatrix} = \begin{bmatrix} 0 & 0 & 1 \\ 0 & \frac{3p\varphi_f}{2} & 0 \end{bmatrix} \begin{bmatrix} i_d \\ i_q \\ \omega_r \end{bmatrix} \quad (8)$$

This model includes electrical and mechanical dynamics and is well-suited for real-time simulation and advanced motor control applications.

3. ADRC Controller for Stator Currents Loop

This paper presents the Active Disturbance Rejection Control (ADRC) method, focusing on applying a linear ADRC controller to first-order inertia systems, as in Equation (9). It explores how the ADRC technique can effectively manage disturbances, enhancing the system's performance and stability. Figure 1 shows a block diagram of ADRC control of the first-order inertia system.

$$P(s) = \frac{y(s)}{u(s)} = \frac{K}{Ts+1} \Longrightarrow T.\dot{y}(t) + y(t) = Ku(t) \quad (9)$$

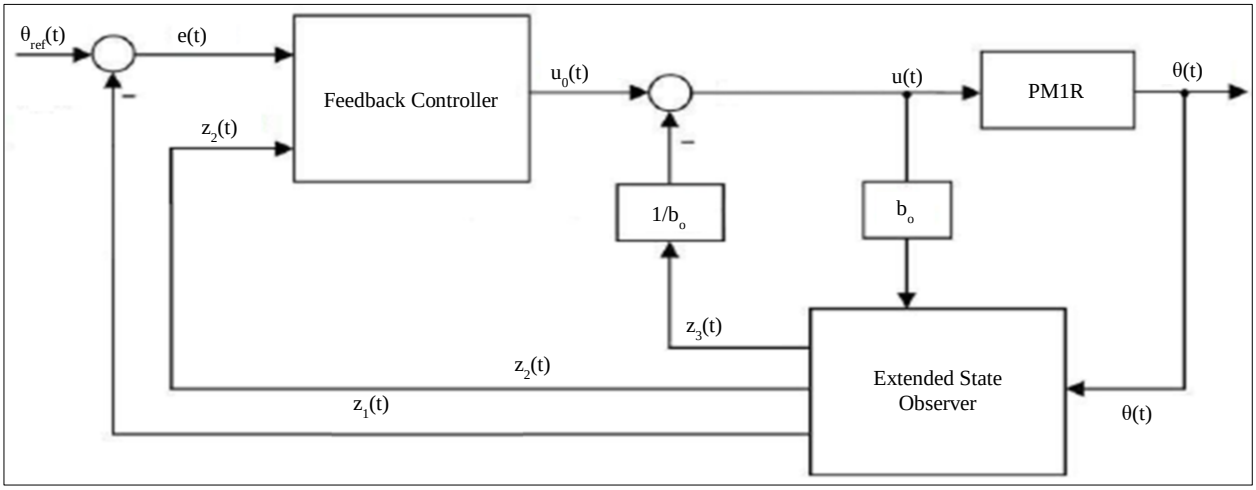

Fig. 1 A block diagram of ADRC control [9]

The ADRC for first-order systems comprises essential elements like the Tracking Differentiator (TD) and a regulator to estimate and counteract disturbances and dynamics. This structure enhances the system's response to disturbances and uncertainties during control.

Designing a linear ADRC controller for a first-order object involves four essential steps.

- Model: Determine the coefficient b_0 For a first-order object with the given transfer function $P(s) = \frac{K}{Ts+1}$.
- Control structure: Construct a proportional controller with extended observer and noise rejection, such as:

$$\begin{pmatrix} \dot{\widehat{x_1}}(t) \\ \dot{\widehat{x_2}}(t) \end{pmatrix} = \begin{pmatrix} -l_1 & 1 \\ -l_2 & 0 \end{pmatrix} \begin{pmatrix} \widehat{x_1}(t) \\ \widehat{x_2}(t) \end{pmatrix} + \begin{pmatrix} b_0 \\ 0 \end{pmatrix} u(t) + \begin{pmatrix} l_1 \\ l_2 \end{pmatrix} y(t) \quad (11)$$

$$u(t) = \frac{K_p(r(t)+\widehat{x_1}(t))-\widehat{x_2}(t)}{b_0} \quad (10)$$

Closed-loop dynamics: Select $K_p = \frac{4}{T_{2\%}}$

Observer dynamics: Position the observer's pole to the left of the closed-loop pole.

$l_1 = -2.s^{ESO}$, $l_2 = (s^{ESO})^2$ with $s^{ESO} \approx (2 \dots 19)s^{CL}$, and $s^{CL} = -K_p$

This leads to the ADRC control structure for a first-order object represented by Equation (11):

$$y(t) = K_I u(t) \Longrightarrow P(s) = \frac{y(s)}{u(s)} = \frac{K_I}{s} \quad (11)$$

Assuming an input disturbance of 0 and where b is the unknown component of IK, reformulated as in Equation (12).

$$\dot{y}(t) = \big(d(t) + \Delta b.u(t)\big) + b_0.u(t) = f(t) + b_0.u(t) \quad (12)$$

In the IM motor current model, because the dq coordinate system has the real axis d, it coincides with the rotor flux axis, so $\varphi_{\boldsymbol{q}} = 0$. The mathematical model of a PMSM will be rewritten as Equation (13):

$$\frac{di_d}{dt} = -\left(\frac{1}{\sigma T_s} + \frac{1-\sigma}{\sigma T_r}\right) i_d + \omega_{\boldsymbol{s}} i_q + L_m \frac{1-\sigma}{\sigma T_r} \varphi_{\boldsymbol{d}} + \frac{1}{\sigma L_s} u_d$$

$$\frac{di_{\boldsymbol{q}}}{dt} = -\left(\frac{1}{\sigma T_s} + \frac{1-\sigma}{\sigma T_r}\right) i_{\boldsymbol{q}} - \omega_{\boldsymbol{s}} i_d - L_m \omega \frac{1-\sigma}{\sigma T_r} + \frac{1}{\sigma L_s} u_{\boldsymbol{q}}$$

$$\frac{d\varphi_d}{dt} = \frac{L_m}{T_r} i_d - \frac{L_m}{T_r} \varphi_{\boldsymbol{d}} \quad (13)$$

Design separate ESO for each input and output pair as follows. Consider the first state as follows:

$$\dot{i_d} = -\left(\frac{1}{\sigma T_s} + \frac{1-\sigma}{\sigma T_r}\right) i_d + \omega_{\boldsymbol{s}} i_q + L_m \frac{1-\sigma}{\sigma T_r} \varphi_{\boldsymbol{d}} + \frac{1}{\sigma L_s} u_d = f(t) + b_{10}.u(t) \quad (14)$$

with $b_{10} \frac{1}{\sigma L_s}$

The state equation of the extended state observer ESO1 and the control law:

$$\begin{pmatrix} \dot{\widehat{x_1}}(t) \\ \dot{\widehat{x_2}}(t) \end{pmatrix} = \begin{pmatrix} -l_1 & 1 \\ -l_2 & 0 \end{pmatrix} \begin{pmatrix} \widehat{x_1}(t) \\ \widehat{x_2}(t) \end{pmatrix} + \begin{pmatrix} b_0 \\ 0 \end{pmatrix} u(t) + \begin{pmatrix} l_1 \\ l_2 \end{pmatrix} y(t)$$

$$u(t) = \frac{K_p(r_{\boldsymbol{1}}(t)+\widehat{y_1}(t))-\hat{f}(t)}{b_{10}} = \frac{K_{p1}(r_{\boldsymbol{1}}(t)+\widehat{x_{11}}(t))-\widehat{x_{12}}(t)}{b_{10}} \quad (15)$$

With $y_1(t) = \frac{4}{T_1}$=-200

Choose the transition time $y_1$according to T_1=0,02(s); $K_{\mathrm{p1}}\frac{4}{T_1}$=200. The pole positions of the observer and the closed loop are calculated as follows:

$$s^{CL} = -K_{p1} = -200 \quad (16)$$

With: $s^{ESO} = 10s^{CL} = -200$

Therefore

$$\begin{cases} l_{11} = -2s^{ESO} = 4000 \\ l_{12} = (s^{ESO})^2 = -2000^2 \end{cases} \quad (17)$$

Therefore, the parameter of the ADRC 1 for the first state is:

$$\begin{cases} K_{\mathrm{P1}} = 200 \\ l_{11} = 4000 \\ l_{12} = 2000^2 \end{cases} \quad (18)$$

Similarly calculating for the second state, we get the parameter of the ADRC 2 as follows:

$$\begin{cases} K_{\mathrm{P2}} = 20 \\ l_{11} = 4000 \\ l_{12} = 2000^2 \end{cases} \quad (19)$$

4. ADRC Controller for Speed Loop

In the speed model for an IM motor, Equation (20). Equation (20) provides a mathematical representation of the dynamic relationship between the electromagnetic torque and the rotor speed.

$$\frac{d\omega_r}{dt} = -\frac{1}{J}T_m + \frac{3}{2}p\frac{L_m}{L_r}\varphi_f i_q\frac{1}{J} = -\frac{1}{J}T_m + \ K.i_q$$

$$= f_3(t) + b_{30}u_3(t) \quad (20)$$

With $u_3(t) = i_{\mathrm{q}}(t)$; $y_3(t) = \omega(t)$; $T_3 = 0{,}1(s)$; $K_{p1} = 40$.

The pole positions of the observer and the closed loop are calculated as follows:

$$s^{CL} = -K_{p1} = -40$$

With: $s^{ESO1} = 10s^{CL} = -400$

$$\begin{cases} l_{11} = -2s^{ESO} = 800 \\ l_{12} = (s^{ESO})^2 = -400^2 \end{cases} \quad (21)$$

Therefore, the parameter of the ADRC3 for the first state as Equation (22).

$$\begin{cases} K_{\mathrm{P1}} = 40 \\ l_{11} = 800 \\ l_{12} = 400^2 \end{cases} \quad (22)$$

5. Simulation Results

Table 1 lists the key IM motor parameters: rated power, voltage, stator and rotor resistance, magnetising inductance, and leakage inductance. These specifications are vital for analysing the motor's performance and dynamics, enabling precise modelling and simulation for various applications.

Table 1. The parameter of the induction motor

Parameters	Units	Values
Stator resistance	Ω	0,787
Rotor resistance	Ω	1,57
Stator inductance	H	0,00177
Rotor inductance	H	0,00178
Capacity of motor	kW	2
Number of Pole Pair		1
Speed motor	Rpm	2850

The paper uses MATLAB simulations with ADRC1, ADRC2, and ADRC3 controller parameters, as in part 3—Figures 2, 3, and 4 present the stator current, speed, and torque responses. Comparing the controllers reveals progressive performance improvements. ADRC1 provides acceptable control but shows slower responses and larger overshoots in torque and acceleration.

ADRC2 enhances transient and steady-state behaviour, reducing overshoots and achieving faster settling times. ADRC3 delivers optimal performance with minimal overshoot, rapid convergence, and improved disturbance rejection.

Figure 2 shows the stator current responses i_d , i_q, while Figure 3 shows the speed response. The i_d , i_q currents demonstrate a rapid transient response, settling to their reference values with minimal overshoot. This highlights the effectiveness of the implemented control strategy in maintaining precise current regulation.

Figure 2 indicates a positive stator response. The flux control current (i_d) varies during stable motor operation, confirming that the flux response remains constant, which allows for smooth engine operation. The speed control current performs well during the starting process at t=3s, peaking at 6,8A before gradually decreasing to enhance speed.

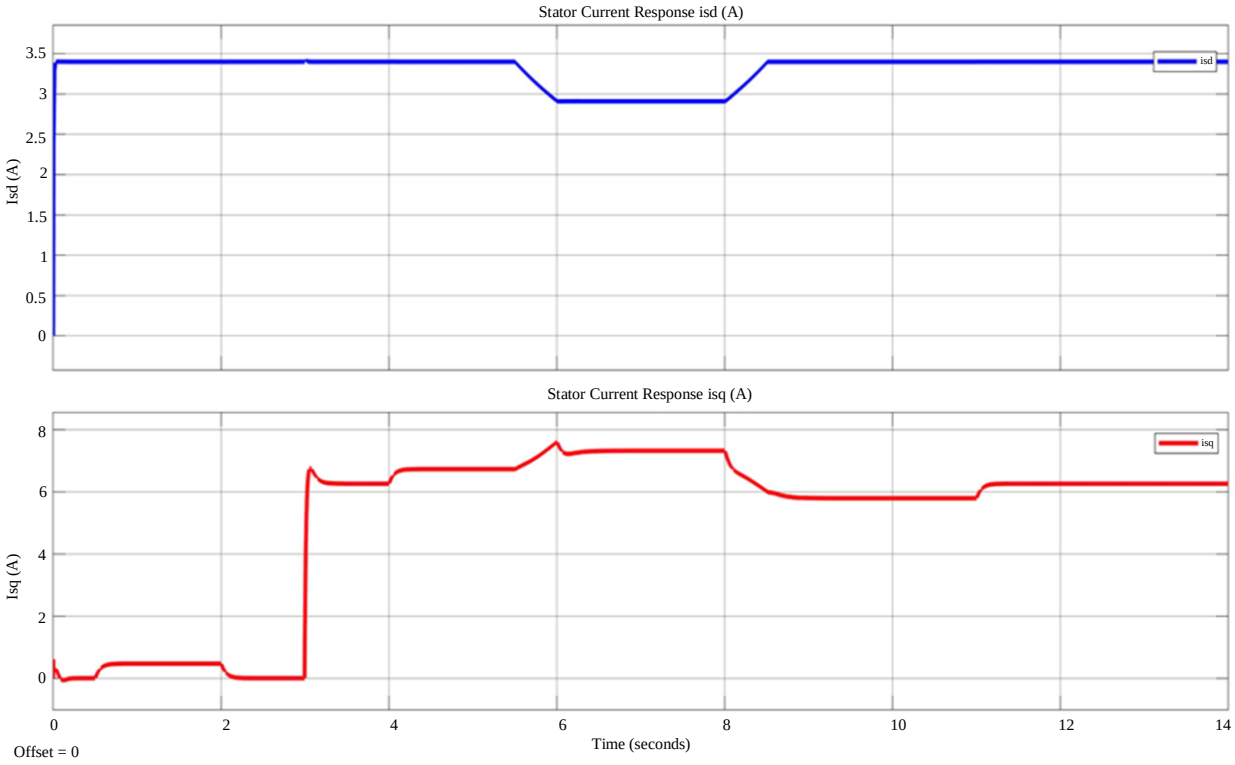

Fig. 2 The stator current responses

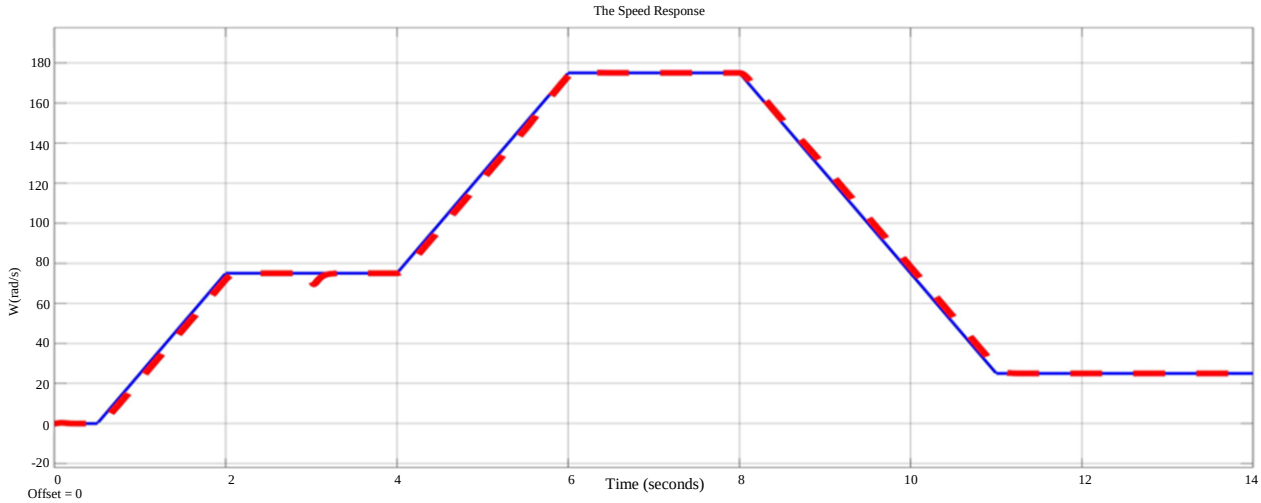

Fig. 3 The speed response

Furthermore, there is no over-regulation in the stator currents during transitions, although both currents overlap for 0.5s when load torque is applied to the system. The analysis underscores the effective control strategy for managing the motor's performance. The flux control current is consistent, and it is a well-tuned system that minimises fluctuations, thereby ensuring efficient power utilisation. During the steady-state phase, the motor's operational stability is further evidenced by the minimal deviations $i_d and$ affirming that conditions remain favourable for sustained performance.

Figure 3 illustrates the motor's speed response. The ADRC algorithm ensures the motor follows the set speed without load. At t=3s, the speed drops when a load is applied but quickly stabilises, demonstrating the algorithm's robustness against disturbances. Despite the sustained load, the motor maintains a nearly constant speed, showcasing effective disturbance rejection. When the load is removed at t=6s, the speed temporarily overshoots but swiftly returns to the setpoint, highlighting the system's precise handling of transient and steady-state conditions.

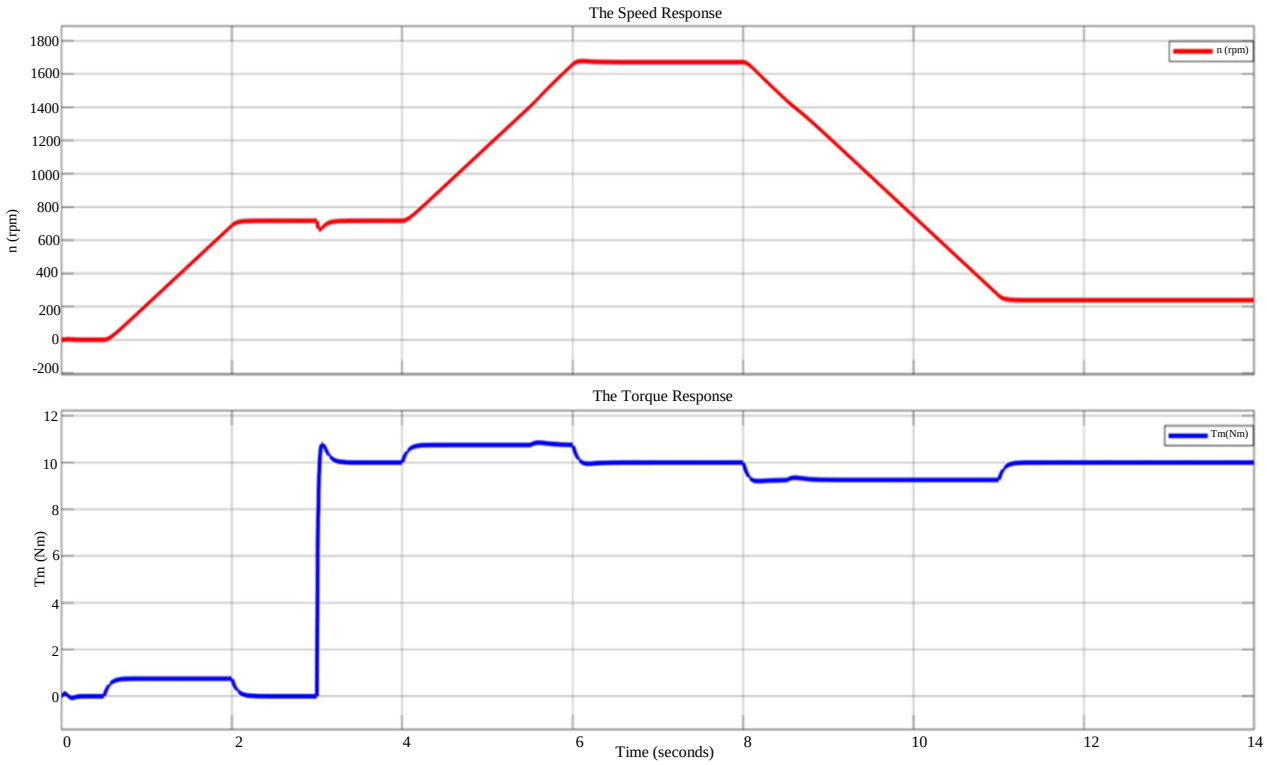

Fig. 4 The speed and torque responses

Figure 4 illustrates the simulation results of the motor torque response, which closely mirrors the iq current response. The torque varies with different motor speed scenarios. During transient conditions (such as starting or applying load torque), the torque briefly increases, while stable operation maintains a consistent torque level. However, there is a slight overshoot of 3% during these transient periods. This behaviour can be attributed to the dynamic characteristics of the motor control system, which aims to optimise performance in response to varying operational demands. As depicted in Figure 2, Figure 4, the iq current, which directly influences torque generation, exhibits an immediate reaction to changes in load. This correlation underlines the importance of precise current control to minimise response time and enhance torque stability.

6. Conclusion

This research initially focused on using an active controller to eliminate ADRC noise for controlling channel separation in three-phase asynchronous motors. The favourable control results indicate that the ADRC method promises future development. However, due to constraints in capacity and time, the findings have limitations, including the need for sensors for signal measurement and feedback and the absence of experimental validation. Addressing these issues will provide a foundation for more comprehensive research and development in the future. Future research should prioritise integrating advanced sensor technologies to facilitate real-time signal measurement and feedback mechanisms. This enhancement will improve the accuracy of the ADRC implementation and enable the collection of critical data for further analysis. Additionally, conducting experimental validation in controlled environments is essential to assess the practical applicability of the ADRC method in various operational scenarios. Moreover, exploring the ADRC approach's scalability in larger systems could yield insights into its effectiveness across different motor configurations.

References

[1] Yi Huang, and Wenchao Xue, "Active Disturbance Rejection Control: Methodology and Theoretical Analysis," *ISA Transactions*, vol. 53, no. 4, pp. 963-976. 2014. [CrossRef] [Google Scholar] [Publisher Link]

[2] Jingqing Han, "From PID to Active Disturbance Rejection Control," *IEEE Transactions on Industrial Electronics*, vol. 56, no. 3, pp. 900-906, 2009. [CrossRef] [Google Scholar] [Publisher Link]

[3] Jie Li et al., "Active Disturbance Rejection Control: Theoretical Results Summary and Future Researches," *Control Theory and Applications*, vol. 34, no. 3, pp. 281-295. 2017. [CrossRef] [Google Scholar] [Publisher Link]

[4] Mingwei Sun et al., "Application and Analysis of ADRC in Guidance and Control in Flight Vehicle—some Explorations in Various Time-Scale Paradigms," *Proceedings of the 29th Chinese Control Conference*, Beijing, China, 2010. [Google Scholar] [Publisher Link]

[5] A. De Luca, and G. Ulivi, "Design of an Exact Nonlinear Controller for Induction Motors," *IEEE Transactions on Automatic Control*, vol. 34, no. 12, pp. 1304-1307, 1989. [CrossRef] [Google Scholar] [Publisher Link]

[6] Abderrahim Bentaallah et al., "Adaptive Feedback Linearization Control for Asynchronous Machine with Nonlinear for Natural Dynamic Complete Observer," *Journal of Electrical Engineering*, vol. 63, no 2, pp. 88-94, 2012. [CrossRef] [Google Scholar] [Publisher Link]

[7] Jingqing Han, "From PID to Active Disturbance Rejection Control," *IEEE Transactions on Industrial Electronics*, vol. 56, no. 3, pp. 900-906, 2009. [CrossRef] [Google Scholar] [Publisher Link]

[8] Gernot Herbst, "A Simulative Study on Active Disturbance Rejection Control (ADRC) as a Control Tool for Practitioners," *Electronic*, vol. 2, no. 3, pp. 246-279, 2013. [CrossRef] [Google Scholar] [Publisher Link]

[9] R. Gregor et al., "Enhanced Predictive Current Control Method for the Asymmetrical Dual – Three Phase Induction Machine," *2009 IEEE International Electric Machines and Drives Conference*, Miami, FL, USA, 2009. [CrossRef] [Google Scholar] [Publisher Link]

[10] Zixin Li et al., "Improved Active Disturbance Rejection Control of Permanent-Magnet Synchronous Motor Based on BP Neural Network," *2020 23rd International Conference on Electrical Machines and Systems (ICEMS)*, Hamamatsu, Japan, 2020. [CrossRef] [Google Scholar] [Publisher Link]

[11] Ping Lin et al., "A Class of Linear-Nonlinear Switching Active Disturbance Rejection Speed and Current Controllers for PMSM," *IEEE Transactions on Power Electronics*, vol. 36, no. 12, pp. 14366-14382, 2021. [CrossRef] [Google Scholar] [Publisher Link]

[12] Lizhi Qu, Wei Qiao, and Liyan Qu, "Active-Disturbance-Rejection-Based Sliding-Mode Current Control for Permanent-Magnet Synchronous Motors," *IEEE Transactions on Power Electronics*, vol. 36, no. 1, pp. 751-760, 2021. [CrossRef] [Google Scholar] [Publisher Link]

[13] Patel, Dixitbhai, and Lin Zhao, "Active disturbance Rejection Control of Doubly-Fed Induction Generator during Voltage Dip," *Proceedings of ESA Annual Meeting on Electrostatics*, 2010. [Google Scholar]

[14] Francesco Alonge et al., "Robust Active Disturbance Rejection Control of Induction Motor Systems Based on Additional Sliding Mode Component," *IEEE Transactions on Industrial Electronics*, vol. 64, no.7, pp. 5608-5621, 2017. [CrossRef] [Google Scholar] [Publisher Link]